In-Line Waveguide Selective Linear Phase Filters

JOHN DAVID RHODES, MEMBER, IEEE, AND M. ZAWAWI ISMAIL

Abstract—**A procedure is described whereby narrow-band waveguide selective linear phase filters may be designed from a low-pass prototype linear phase network. The structure is comprised of a cascade connection of basic sections, each containing a direct-coupled cavity together with a dual-mode resonator. Each dual-mode resonator takes the form of a square guide mounted on the broad wall of the main rectangular guide and coupled to this guide by a small aperture. Explicit formulas for the susceptance of the coupling apertures and electrical lengths of the cavities are given in terms of the low-pass prototype.**

Introduction

THERE ARE many techniques suitable in the design of microwave filters from the conventional minimum-phase low-pass prototype filters. In waveguides, the half-wave direct-coupled cavity filters provide a good compact structure [1]. Recently, some new design techniques have been developed for the low-pass prototype selective linear phase filters in a multipath form, with microwave realizations [2]–[4].

More recently, a cascade synthesis procedure has been developed for the same class of filters with application to lumped-element bandpass channel filters [5]. In the low-pass prototype, the transmission zeros were extracted using second-degree sections which inherently contain frequency invariant reactances. In this paper, a new design technique is presented for narrow-band waveguide selective linear phase filters based upon this low-pass prototype selective linear phase filter.

Initially, the properties of the low-pass prototype network are briefly discussed, and the design procedure developed and illustrated by experimental results.

The Low-Pass Prototype Linear Phase Filter

A possible scattering transfer function of a $(2n+1)$ degree network of a low-pass selective linear phase prototype has been shown to be

$$S_{12}(p) = \frac{Ev[p_n(-p/\epsilon)[2P_{n+1}(p/\epsilon) - P_n(p/\epsilon)]]}{P_n(p/\epsilon)[2P_{n+1}(p/\epsilon) - P_n(p/\epsilon)]} \quad (1)$$

where $P_n(p/\epsilon)$ is the equidistant linear phase polynomial[1] defined through the degree varying recurrence formula.

$$P_{n+1}(p/\epsilon) = P_n(p/\epsilon) + \left(\frac{\tan\epsilon}{\epsilon}\right)^2 \frac{\{p^2 + (\epsilon n)^2\}}{(4n^2-1)} P_{n-1}(p/\epsilon)$$

with the initial conditions

$$P_0(p/\epsilon) = 1, \qquad P_1(p/\epsilon) = 1 + \left(\frac{\tan\epsilon}{\epsilon}\right) p \quad (2)$$

where ϵ varies the passband ripple level.

From (1) and (2), we may construct $S_{11}(p)$ to be of the form

$$S_{11}(p) = A_n \prod_1^n (p^2 + \epsilon^2 m^2)/P_n(p/\epsilon)[2P_{n+1}(p/\epsilon) - P_n(p/\epsilon)]$$

where

$$A_n = \left(\frac{\tan\epsilon}{\epsilon}\right)^{2n+1} 2 \Big/ (2n+1) \prod_1^n (2n-1)^2. \quad (3)$$

Normalizing the generator impedance to unity, the input admittance $Y(p)$ becomes

$$Y(p) = \frac{1 - S_{11}(p)}{1 + S_{11}(p)}. \quad (4)$$

The synthesis of this admittance function $Y(p)$ in the manner described in [5] leads to the network shown in Fig. 1, which is designed to exhibit complex conjugate symmetry. A table of element values for the maximally flat case was also given previously in [5]. A similar but improved performance may be obtained using modified forms of this transfer function [8], [9].

The Design Procedure

The in-line waveguide selective linear phase filter is shown in Fig. 2 and is defined according to the normalized midband susceptances and electrical lengths as depicted in Fig. 3. The design procedure is based upon equating this structure at midband to the low-pass prototype linear phase filter.

Initially, consider the section consisting of two inductive susceptances each symmetrically embedded in a negative length of transmission line separated by a length of transmission line of electrical length θ_r, shown in Fig. 4. Each inductive susceptance embedded in the negative length of line may be approximated by a frequency-dependent immittance inverter, while the length of transmission line of electrical length θ_r can be represented by

Manuscript received October 19, 1972; revised July 16, 1973.
The authors are with the Department of Electrical and Electronic Engineering, University of Leeds, Leeds, England.

[1] Phase deviation from linearity is zero at periodically spaced frequency increments.

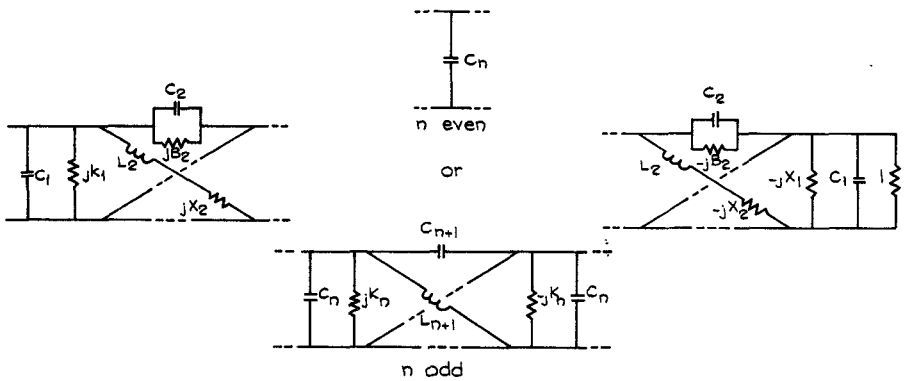

Fig. 1. Low-pass prototype network for the odd-degree selective linear phase filter.

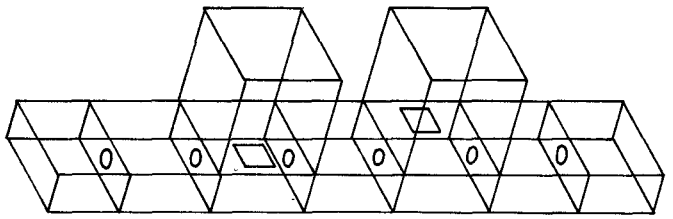

Fig. 2. The in-line waveguide linear phase filter.

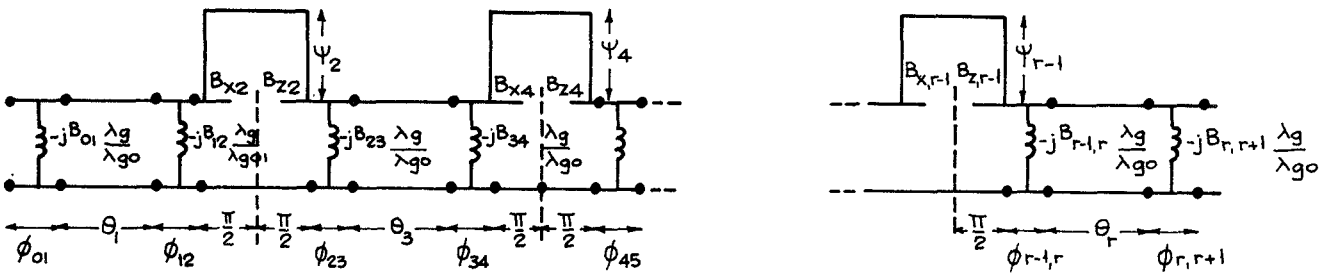

Fig. 3. Midband susceptances and electrical lengths defining the in-line waveguide linear phase filter.

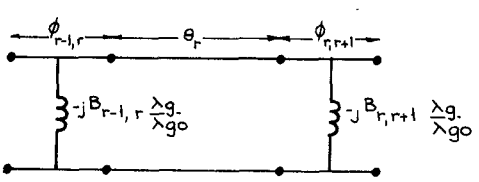

Fig. 4. Two shunt inductive susceptances between a length of transmission line.

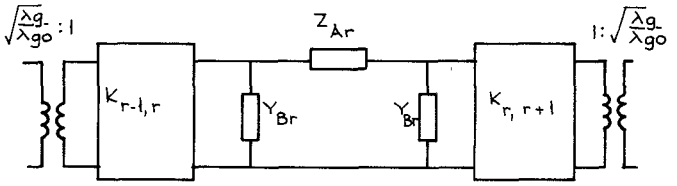

Fig. 5. Approximate equivalent circuit for the coupled-cavity of Fig. 4.

an equivalent pi-section [4]. Thus the equivalent circuit for Fig. 4 is that shown in Fig. 5, where

$$B_{r-1,r} = K_{r-1,r} - 1/K_{r-1,r}$$

$$\phi_{r-1,r} = \cot^{-1}\left(\frac{B_{r-1,r}}{2}\right) \tag{5}$$

and

$$Z_{Ar} = -j\frac{\lambda_g}{\lambda_{g0}}\sin\left(\theta_r\frac{\lambda_{g0}}{\lambda_g}\right)$$

$$Y_{Br} = -j\frac{\lambda_{g0}}{\lambda_g}\cot\left(\frac{\theta_r}{2}\frac{\lambda_{g0}}{\lambda_g}\right).$$

(For narrow bandwidths, $K \gg \theta/2$ around $\lambda_g = \lambda_{g0}$ and, therefore, the shunt elements may be neglected [1].)

Next, consider a dual-mode resonator between two quarter-wavelength transmission lines, Fig. 6. An exact analysis of the dual-mode resonator is difficult to obtain. An approximation based on the small aperture theory [6] can be derived, from which the equivalent circuit of the dual-mode resonator can be obtained. Using this technique, assuming only the dominant TE_{01} and TE_{10} modes propagate in the square guide, the equivalent circuit of Fig. 6 is that shown in Fig. 7, where

$$X_{Ar}' = \left[\frac{B_{Ar}\sin(\pi/2)(\lambda_{g0}/\lambda_g) - \cos(\pi/2)(\lambda_{g0}/\lambda_g)}{\sin(\pi/2)(\lambda_{g0}/\lambda_g) - B_{Ar}\cos(\pi/2)(\lambda_{g0}/\lambda_g)}\right]$$

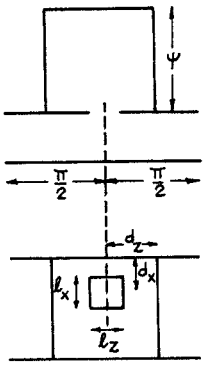

Fig. 6. Dual-mode resonator.

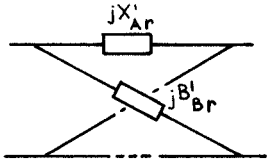

Fig. 7. Lattice equivalent circuit for the dual-mode resonator.

$$B_{Br}' = \left[\frac{X_{Br}\sin(\pi/2)(\lambda_{g0}/\lambda_g) - \cos(\pi/2)(\lambda_{g0}/\lambda_g)}{\sin(\pi/2)(\lambda_{g0}/\lambda_g) - X_{Br}\cos(\pi/2)(\lambda_{g0}/\lambda_g)}\right] \quad (6)$$

and

$$B_{Ar} = \frac{-b/a}{\sin^4(\pi d_{xr}/a)}\left[\cot\psi_r\frac{\lambda_{g0}}{\lambda_g} + B_{xr}\frac{\lambda_g}{\lambda_{g0}}\right]$$

$$X_{Br} = \frac{-4ab}{\lambda_g^2\cos^2(\pi d_{xr}/a)\sin^2(\pi d_{xr}/a)}\left[\cot\psi_r\frac{\lambda_{g0}}{\lambda_g} + B_{xr}\frac{\lambda_g}{\lambda_{g0}}\right].$$

Considering the above results, the equivalent circuit for the waveguide filter shown in Fig. 2 is that shown in Fig. 8, where the transformers of turns ratios $(\lambda_g/\lambda_{g0})^{1/2}$ and $(\lambda_{g0}/\lambda_g)^{1/2}$ are eliminated, and we have

$$Z_r = -j\frac{\lambda_g}{\lambda_{g0}}\sin\theta_r\frac{\lambda_{g0}}{\lambda_g} \quad (7)$$

and

$$Z_{Ar} = j\frac{\lambda_g}{\lambda_{g0}}X_{Ar}'$$

$$Y_{Br} = j\frac{\lambda_{g0}}{\lambda_g}B_{Br}'.$$

The low-pass prototype shown in Fig. 1 may be transformed into the network shown in Fig. 8 by first introducing unity immittance inverters so that the shunt capacitances together with frequency invariant susceptances are transformed into series inductors and frequency invariant reactances, and then transforming the admittance level at each node to yield equal-valued inductors where $\alpha \gg 1$. The network is shown in Fig. 9, where

$$C_i' = \frac{1}{\alpha}, \qquad B_i' = \frac{B_i}{L_i\alpha}$$

$$L_i' = C_iL_i\alpha, \qquad X_i' = B_iL_i\alpha.$$

We then apply the frequency transformation

$$\omega \rightarrow \alpha\frac{\lambda_g}{\lambda_{g0}}\sin\left(\frac{\pi\lambda_{g0}}{\lambda_g}\right) \quad (8)$$

and we equate the networks at midband. For the iris-coupled cavity, we have

$$-\frac{\lambda_g}{\lambda_{g0}}\sin\pi\frac{\lambda_{g0}}{\lambda_g} + \frac{K_r'}{\alpha C_r} \approx -\frac{\lambda_g}{\lambda_{g0}}\sin\theta_r\frac{\lambda_{g0}}{\lambda_g}. \quad (9)$$

Equating the functions at $\lambda_g = \lambda_{g0}$ we have

$$\theta_r = \pi - \sin^{-1}\frac{K_r'}{C_r\alpha}. \quad (10)$$

Equating the values of the impedance inverter

$$K_{r,r+1} = Y_{r,r+1}. \quad (11)$$

To a second degree of approximation, the frequency transformation (8) reduces to

$$\omega \rightarrow \alpha\pi(1 - \lambda_g/\lambda_{g0}). \quad (12)$$

If λ_{g1} and λ_{g2} are the guide wavelengths corresponding to the required bandedge frequencies f_1 and f_2, the

$$\lambda_{g0} = \frac{\lambda_{g1} + \lambda_{g2}}{2}$$

and

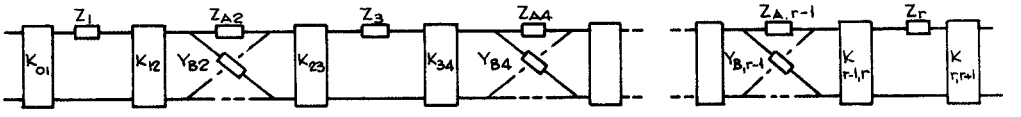

Fig. 8. Equivalent circuit for the in-line waveguide linear phase filter.

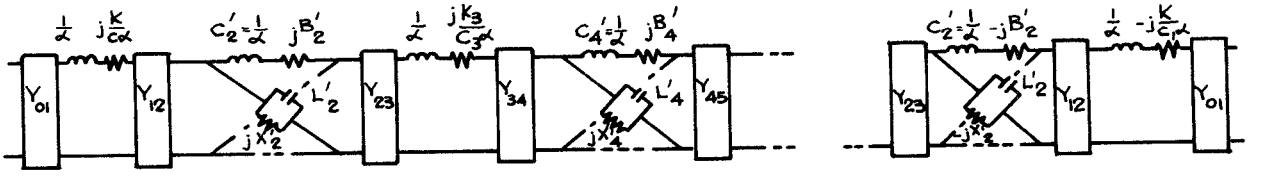

Fig. 9. Low-pass prototype network after admittance scaling.

$$\alpha = \frac{\omega'(\lambda_{g1} + \lambda_{g2})}{\pi(\lambda_{g1} - \lambda_{g2})} \tag{13}$$

where ω' is the cutoff frequency of the low-pass prototype [4].

Applying the transformation (12) to the lattice elements, and approximately equating the lattice arm immittances to the equivalent lattice of the dual-mode resonator, we have, for the series arm impedance,

$$\frac{\lambda_g}{\lambda_{g0}}\left[\frac{B_{Ai}\sin(\pi/2)(\lambda_{g0}/\lambda_g) - \cos(\pi/2)(\lambda_{g0}/\lambda_g)}{\sin(\pi/2)(\lambda_{g0}/\lambda_g) - B_{Ai}\cos(\pi/2)(\lambda_{g0}/\lambda_g)}\right]$$

$$\approx \pi\left(1 - \frac{\lambda_g}{\lambda_{g0}}\right) + \frac{X_i}{L_i\alpha} \tag{14}$$

where

$$B_{Ai} = \frac{-b/a}{\sin^4(\pi d_{xi}/a)}\left[\cos\psi_r\frac{\lambda_{g0}}{\lambda_g} + B_{xi}\frac{\lambda_g}{\lambda_{g0}}\right].$$

Equating the functions and derivatives at $\lambda_g = \lambda_{g0}$ we have

$$\frac{b/a}{\sin^4(\pi d_{xi}/a)}[\cot\psi_i + B_{xi}] = \frac{X_i}{L_i\alpha}$$

$$\frac{b/a}{\sin^4(\pi d_{xi}/a)}[\psi_i\csc^2\psi_i + B_{xi}]$$

$$= \pi + \frac{\pi}{2}\left\{1 + \left(\frac{X_i}{L_i\alpha}\right)^2\right\} - \frac{X_i}{L_i\alpha}. \tag{15}$$

For the shunt arm admittance,

$$\frac{\lambda_{g0}}{\lambda_g}\left[\frac{X_{Bi}\sin(\pi/2)(\lambda_{g0}/\lambda_g) - \cos(\pi/2)(\lambda_{g0}/\lambda_g)}{\sin(\pi/2)(\lambda_{g0}/\lambda_g) - X_{Bi}\cos(\pi/2)(\lambda_{g0}/\lambda_g)}\right]$$

$$\approx C_iL_i\alpha^2\left(1 - \frac{\lambda_g}{\lambda_{g0}}\right) + B_iL_i\alpha \tag{16}$$

where

$$X_{Bi} = \frac{-4ab}{\lambda_g^2\cos^2(\pi d_{xi}/a)\sin^2(\pi d_{zi}/a)}\left[\cot\psi_i\frac{\lambda_{g0}}{\lambda_g} + B_{zi}\frac{\lambda_g}{\lambda_{g0}}\right].$$

Again equating the functions and derivatives at midband we have

$$\frac{4ab}{\lambda_{g0}^2\cos^2(\pi d_{xi}/a)\sin^2(\pi d_{zi}/a)}[\cot\psi_i + B_{zi}] = B_iL_i\alpha$$

and

$$\frac{4ab}{\lambda_{g0}^2\cos^2(\pi d_{xi}/a)\sin^2(\pi d_{zi}/a)}[\psi_i\csc^2\psi_i - B_{zi} - 2\cot\psi_i]$$

$$= L_iC_i\alpha^2\pi + \frac{\pi}{2}\{1 + (B_iL_i\alpha)^2\} + B_iL_i\alpha. \tag{17}$$

Subtracting (15), we obtain

$$\psi_i\csc^2\psi_i - \cot\psi_i$$

$$= \sin^4\frac{\pi d_{xi}}{a}\frac{a}{b}\left[\pi + \frac{\pi}{2}\left\{1 + \left(\frac{X_i}{L_i\alpha}\right)^2\right\} - \frac{2X_i}{L_i\alpha}\right] \tag{18}$$

while, adding (17), we obtain

$$\psi_i\csc^2\psi_i - \cot\psi_i = \frac{\lambda_{g0}^2}{4ab}\cos^2\frac{\pi d_{xi}}{a}\sin\frac{\pi d_{zi}}{a}$$

$$\cdot\left[L_iC_i\alpha^2\pi + \frac{\pi}{2}\{1 + (B_iL_i\alpha)^2\} + 2B_iL_i\alpha\right]. \tag{19}$$

From (18) and (19) we obtain the condition

$$\sin^4\frac{\pi d_{xi}}{a} = \cos^2\frac{\pi d_{xi}}{a}\sin^2\frac{\pi d_{zi}}{a}\frac{\lambda_g^2}{4a^2}$$

$$\cdot\left[\frac{L_iC_i\alpha^2\pi + (\pi/2)(1 + B_i^2L_i^2\alpha^2) + 2B_iL_i\alpha}{\pi + (\pi/2)\{1 + (X_i/L_i\alpha)^2\} - (2X_i/L_i\alpha)}\right] \tag{20}$$

from which d_{xi}, d_{zi} can be obtained.

Equation (15) may be reduced to

$$2\psi_i - \sin 2\psi_i - (1 - \cos 2\psi_i)$$

$$-\frac{a}{b}\sin^4\frac{\pi d_{xi}}{a}\left[\pi + \frac{\pi}{2}\left\{1 + \left(\frac{X_i}{L_i^2\alpha}\right)^2\right\} - \frac{2X_i}{L_i\alpha}\right] = 0 \tag{21}$$

and ψ_i can be obtained by an iterative method. B_{xi} and B_{zi} can be obtained directly from the first equations in (14) and (16).

Summarizing with respect to the element values of the low-pass prototype given in Fig. 1 and the element values of the equivalent circuit for the waveguide filter given in Fig. 8, we have

$$\alpha = \frac{\omega'(\lambda_{g1} + \lambda_{g2})}{\pi(\lambda_{g1} - \lambda_{g2})}$$

and, for the first half of the network

$$K_{01} = (C_1\alpha)^{1/2}$$

$$K_{i,i+1} = \begin{cases} (C_1L_{i+1}\alpha)^{1/2}, & i = 1,3,5,\cdots,n\ (n\text{ odd}) \\ & \text{or } n+1\ (n\text{ even}) \\ (L_iC_{i+1}\alpha)^{1/2}, & i = 2,4,\cdots,n-1\ (n\text{ odd}) \\ & \text{or } n\ (n\text{ even}) \end{cases}$$

with

$$B_{i,i+1} = K_{i,i+1} - \frac{1}{K_{i,i+1}}$$

$$\phi_{i,i+1} = -\cot^{-1}\frac{B_{i,i+1}}{2} \tag{22}$$

and

$$\theta_i = -\sin^{-1}\frac{K_i}{C_i\alpha}, \qquad i = 1,3,5,\cdots,n\ (n\text{ odd}) \text{ or } n+1\ (n\text{ even}).$$

For $i = 2,4,6,\cdots,n+1$ (n odd) or n (n even)

$$B_{x,i} = -\cot\psi_i + \frac{X_i}{L_i\alpha}\frac{a}{b}\sin^4\frac{\pi d_{xi}}{a}$$

$$B_{z,i} = -\cot\psi_i + B_iL_i\alpha\frac{\lambda_{g0}^2}{4ab}\cos^2\frac{\pi d_{xi}}{a}\sin^2\frac{\pi d_{zi}}{a}$$

with the conditions

$$2\psi_i - \sin 2\psi_i - (1 - \cos 2\psi_i) \cdot \frac{a}{b} \sin^4 \frac{\pi d_{xi}}{a} \left[\pi + \frac{\pi}{2} \left\{ 1 + \left(\frac{X_i}{L_i \alpha} \right)^2 \right\} - \frac{2X_i}{L_i \alpha} \right] = 0$$

and

$$\sin^4 \frac{\pi d_{xi}}{a} = \frac{\lambda_{g0}}{4a^2} \cos^2 \frac{\pi d_{xi}}{a} \sin^2 \frac{\pi d_{zi}}{a} \cdot \left[\frac{L_i C_i \alpha^2 \pi + (\pi/2)(1 + B_i^2 L_i^2 \alpha^2) + 2B_i L_i \alpha}{\pi + (\pi/2)\{1 + (X_i/L_i\alpha)^2\} - (2X_i/L_i\alpha)} \right].$$

The second half of the network is obtained from the complex conjugate symmetry, i.e., all the frequency invariant immittances are replaced by their conjugates in all the expressions of (22).

Experimental Filter

An experimental waveguide selective linear phase filter was constructed to operate in X band at the center frequency of 9 GHz and with a relative bandwidth of 1 percent, based on the fifth-degree equidistant linear phase low-pass prototype network. Aperture dimensions were obtained from available graphs [7]. For the dual-mode resonator, rectangular apertures were used.

The measured response of the constructed filter is shown in Fig. 10 and the performance summarized as follows:

$$f_0 = 9 \text{ GHz}.$$

Passband

$F_0 \pm 50$ MHz
midband loss, 1.5 dB (unplated)
return loss, 22 dB
delay, 12 ns

Band (Percent)	Insertion Loss Deviation (dB)	Delay Deviation (ns)
85	<0.05	±0.1
90	0.1	+0.5
100	0.3	+1.5

Stopband

$f_0 \pm 120$ MHz, $L > 20$ dB
$f_0 \pm 140$ MHz, $L > 30$ dB

which was in good agreement with the theoretical behavior.

Conclusion

A design procedure has been presented whereby the in-line waveguide selective linear phase filter may be constructed from the element values of the low-pass prototype linear phase filter. The resulting structure is relatively compact and its physical construction is more amenable to direct replacement of conventional waveguide filters in existing systems where additional delay equalization is required. Both the generalized direct-coupled cavity and the in-line filter suffer slight dispersion in the passband due to the frequency dependence of the coupling apertures. However, with the cascade prototype, dispersion may be introduced into the prototype [5] to overcome this effect in broader bandwidth cases, although this must be offset against the disadvantage of being more sensitive to iris sizes due to the dual-mode operation.

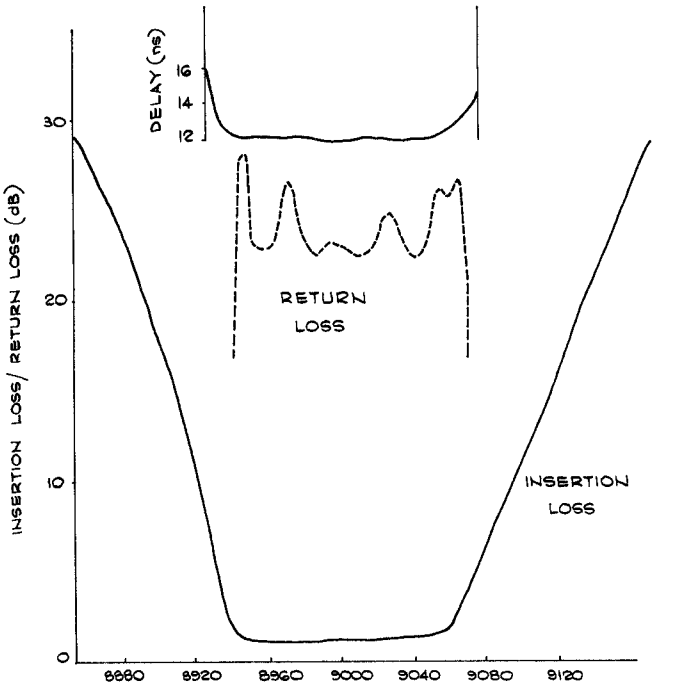

Fig. 10. Measured response of the waveguide linear phase filter based upon the fifth-degree equidistant linear phase prototype.

Finally, it may be noted that the dual-mode cavity may also be realized using a cylindrical cavity instead of a square one [10], and in the derivation of the equivalent circuit for the cylindrical cavity, the dominant TE_{11} modes are assumed.

References

[1] S. B. Cohn, "Direct-coupled-resonator filters," *Proc. IRE*, vol. 45, pp. 187–196, Feb. 1957.
[2] J. D. Rhodes, "A low-pass prototype network for microwave linear phase filters," *IEEE Trans. Microwave Theory Tech.*, vol. MTT-18, pp. 290–301, June 1970.
[3] ——, "The generalized interdigital linear phase filter," *IEEE Trans. Microwave Theory Tech.*, vol. MTT-18, pp. 301–307, June 1970.
[4] ——, "The generalized direct-coupled cavity linear phase filter," *IEEE Trans. Microwave Theory Tech.*, vol. MTT-18, pp. 308–313, June 1970.
[5] J. D. Rhodes and M. Z. Ismail, "Cascade synthesis of selective linear-phase filters," *IEEE Trans. Circuit Theory*, vol. CT-19, pp. 183–189, Mar. 1972.
[6] H. A. Bethe, "Theory of diffraction by small holes," *Phys. Rev.*, vol. 66, pp. 163–182.
[7] G. L. Matthei, L. Young, and E. M. T. Jones, *Microwave Filters, Impedance-Matching Networks, and Coupling Structures*. New York: McGraw-Hill, 1964.
[8] J. D. Rhodes, "Filters with periodic phase delay and insertion loss ripple," *Proc. Inst. Elec. Eng.*, vol. 119, pp. 28–32, Jan. 1972.
[9] ——, "Filters approximating ideal amplitude and arbitrary phase characteristics," *IEEE Trans. Circuit Theory*, vol. CT-20, pp. 120–124, Mar. 1973.
[10] T. A. Abele and H. C. Wang, "An adjustable narrow band microwave delay equalizer," *IEEE Trans. Microwave Theory Tech.*, vol. MTT-15, pp. 566–574, Oct. 1967.